"Sponge-Like" Structures in Polymer Blends: Visualization, Physico-Mathematical Analysis, and Universality

Takeji Hashimoto[*1,2], *Hiroshi Jinnai*[1,a], *Yukihiro Nishikawa*[1,b] *Tsuyoshi Koga*[1,c]

[1]Hashimoto Polymer Phasing Project, ERATO, JST, Japan
[2]Department of Polymer Chemistry, Graduate School of Engineering, Kyoto University, Kyoto 606-8501, Japan

SUMMARY: Mesoscopic structures formed during an ordering process in thermodynamically unstable, isometric, binary molecular mixtures were explored by time-resolved scattering (TRS) and laser scanning confocal microscopy (LSCM). Three-dimensional (3D) bicontinuous structures, which were constructed for the first time by time-resolved LSCM, were found to have a "sponge-like" structure composed of two phases. The structure factor obtained by 3D Fourier transformation of the sponge was found to be identical to that obtained by TRS, confirming that the sponge truly reflects the structural entities evolving in the system. Furthermore, the sponge was shown for the first time to be theoretically predictable by using 3D computer simulations based on the time-dependent Ginzburg-Landau theory. The sponge was subjected to differential geometrical analysis: its Gaussian curvature K, mean curvature H, and their distributions were successfully determined for the first time. The result revealed that the sponge has hyperbolic interfaces with area-averaged curvatures satisfying $<K> < 0$ and $<H> \cong 0$ and that its interface has some deviations from a minimal surface. The sponge was found to be strikingly similar to that occurring in oil/water/surfactant systems at the hydrophile-lipophile-balance, though their characteristic length scales are diversely different (μm vs nm), implying universality of the sponge.

Introduction

Binary mixtures of molecules (or atoms) A and B become thermodynamically unstable, depending on the balance between the cooperative forces associated with intermolecular forces and the forces associated with the entropy of the systems. From a thermodynamic point of view, this instability occurs inside the spinodal curve. The unstable systems undergo phase separation via spinodal decomposition (SD; Ref.1) into two macroscopic phases rich in A and B molecules at thermal equilibrium. The SD process involves the time evolution of phase-separating structures, starting from thermally activated dynamic composition fluctuations of A and B molecules in space (defined as thermal concentration fluctuations) to coexisting domains rich in A and B on a mesoscopic scale (between microscopic and macroscopic scales) and eventually to the two macroscopic phases. This self-organization process of

[a] Present addresses: Department of Polymer Science and Engineering, Kyoto Institute of Technology, Matsugasaki, Kyoto 606-8585, Japan
[b] Structural Biochemistry Laboratory, The Institute of Physical and Chemical Research (RIKEN), 1-1-1 Kouto, Mikaduki, Sayo, Hyogo 679-5148, Japan
[c] Department of Polymer Chemistry, Graduate School of Engineering, Kyoto University, Kyoto 606-8501, Japan

 CCC 1022-1360/00/$ 17,50+.50/0

molecules is one of the themes of non-linear and non-equilibrium phenomena which are left to be answered by modern science.

Many works have been devoted to this non-equilibrium, non-linear phenomenon (Refs. 2-4). One of fundamental questions to be answered is what kind of self-organized structures evolves in mixtures giving rise to two phases which have nearly equal phase-volume (i.e., isometric systems). Experimental studies, in particular time-resolved light scattering (TRLS) studies (one of the method involving the structure analysis in Fourier space), have revealed that the structure evolved is periodic and bicontinuous. The bicontinuity of the structure has been elucidated with the aid of theories (Ref. 5) and computer simulations (Refs. 6,7). The structures evolved at the late stage of SD have been found (Refs. 3,4,8) to obey the dynamic scaling hypothesis (Ref. 9): the evolving structures show a dynamic self-similarity (dynamic fractality) and are primarily scaled with time- and temperature-dependent length scales.

Questions to be answered are: (i) what kind of bicontinuous structures can be expected ? (ii) what is the physical basis of the structures? (iii) how can the structures be characterized mathematically ? (iv) how universal could the structures be ?

To answer question (i), we need to investigate the structures *in situ* and *at real time* using real-space analysis (microscopy methods). Unfortunately, little work along this line has been done up to the present time owing to experimental difficulties. Although many works have been reported on time evolution of scattering structure factors (Fourier-space analysis by scattering methods) (see for example Ref. 3), one cannot visualize real structures directly from the structure factors. To answer question (ii), we should conduct three-dimensional (3D) computer simulations based on a non-linear time evolution equation and find statistical identity between the 3D structures simulated and experimentally determined in real space. Again no work has been reported along this line. To answer question (iii), we should analyze mean principal curvatures and curvature distributions from the mean values for interfaces which separate A-rich and B-rich domains on the basis of differential geometry (see Fig. 1). Again, no work has been reported so far. At the late stage of the SD process the interfaces are well defined and the excess Gibbs energy of our system is localized at the interfaces. Under this situation, *the curvatures of the interfaces and their distributions are the most important information* which characterizes our system. Nevertheless, little information has been available so far because of experimental difficulties. The information should be hidden in the scattering structure factors. However, relationships between the curvature information and the structure factor have not been fully explored. Thus *the curvatures and the structure factors are considered to be essentially independent physical quantities* at the moment. To answer question (iv), we attempted to compare the structures of phase-separating mixtures of simple liquids and polymers with a bicontinuous structure in oil/water/surfactant systems having diversely different physical origin and length scales. No such attempts have been made so far.

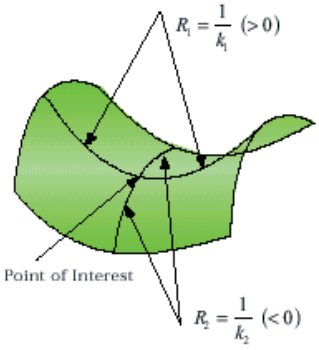

Fig. 1. Definition of two principal curvatures $k_1(\mathbf{r})$ and $k_2(\mathbf{r})$ or mean curvature $H = (k_1 + k_2)/2$ and Gaussian curvature $K = k_1k_2$ at a point of interest located at $\mathbf{r}$ on the interface.

The present work is aimed to explore the four unsolved problems described above and to pioneer a new interdisciplinary problem of chemistry, physics and mathematics with respect to the time evolution of form in soft-condensed matter. We will answer each question below.

What Kind of Bicontinuous Structures Do We Expect to Have ?

In this study we have overcome the experimental difficulties described in the previous section by using polymer mixtures as a model system. We took advantage of polymers having large characteristic lengths and long characteristic times: *large structures grow very slowly in polymer mixtures* as reviewed in Ref. 3. For this purpose we made a lot of effort in chemistry: we synthesized a particular pair of polymers which have a well-defined phase diagram to facilitate the dynamic experiments as described in the previous section. A pair of polymers such as polybutadiene (PB) and polyisoprene (PI) or poly(styrene-*ran*-butadiene) and PB or deuterated PB (dPB) and nondeuterated PB with a narrow molecular weight distribution, were selected as simple hydrocarbon polymers which are amorphous liquids far above glass transition temperature and which exhibit only van der Waals interactions.

We had difficulties investigating 3D periodic, bicontinuous structures with transmission optical microscopy, simply because an overlap of the structures along the depth direction of the sample (i.e., along the incident beam direction) smears real structural entities.
This is one of the primary experimental difficulties in the studies of 3D bicontinuous structures and, in fact, almost no good microscopy studies have been reported so far. We circumvented this difficulty by using laser scanning confocal microscopy (LSCM) (Ref. 10), a recently developed technique which has been applied especially in the field of biology, to our mixtures. The technique enables a 3D scanning of objects and a reconstruction of a 3D image of them. The fact that the time required to capture the 3D image is much shorter than the time scale of the structure growth enables *in situ* observation of 3D optical images.

Figure 2 shows a typical result obtained with LSCM for a polymer mixture at a given time at a late stage of SD (Ref. 11). The figure shows a series of optically sliced images obtained with a focal depth of 0.5 μm and a distance between the successive images of 0.5 μm. The evolving structure is composed of two isometric domains having a spacing about 10 μm: bright domains (domains rich in one polymer) and dark domains (domain rich in the other). The structure grows in size in the time scale of hours, days and years, depending on temperature but the growing structure has dynamic self-similarity (Refs. 3,4,8). In the image at the top-left corner, the dark domain marked **X** is surrounded by the bright domain, thus appearing to be isolated from the neighboring dark domains. However, when we scan the images along the depth direction (corresponding to a shift of the image from a to f), we find that these two dark domains are interconnected in the fourth slice of image d (i.e., 1.5 μm below the first slice).

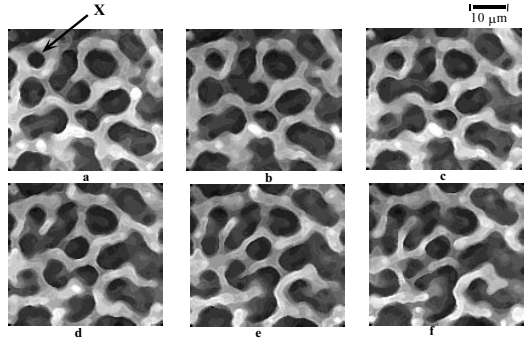

Fig. 2. Optically sliced images taken by laser scanning confocal microscopy (LSCM)

Fig. 2. Optically sliced images taken by laser scanning confocal microscopy (LSCM) of an isometric polymer mixture at a late stage of the SD process. A series of the images were taken at 0.5-μm intervals along the sample thickness direction with focal depth 0.5 μm. The depth where the image is taken increases from a to f.

Thus we find that the two domains are really interconnected and periodically arranged, forming a 3D "maze". We define this characteristic structure as *sponge-like structure* according to the term "sponge" in the field of topology and differential geometry (see, e.g., Ref.12).

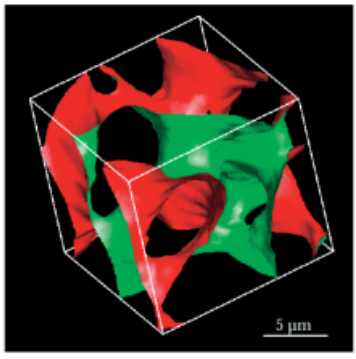

Fig. 3. 3D LSCM image of the interface for the isometric polymer mixture at a late stage of SD having average spacing Λ_m = 12.1 μm (Ref. 13). The bar corresponds to 5 μm.

Figure 3 shows a typical 3D image of the interface constructed by LSCM which separates the two phases, one side of the interface being red and the other green. We can clearly see (i) the bicontinuous feature of the red and green phases, i.e., a 3D continuity of the two phases, and (ii) that most of the interface is saddle-shaped or hyperbolic with $K < 0$. The image in the figure shows the size of one average spacing. The image representing a much larger length scale is shown in Fig. 4.

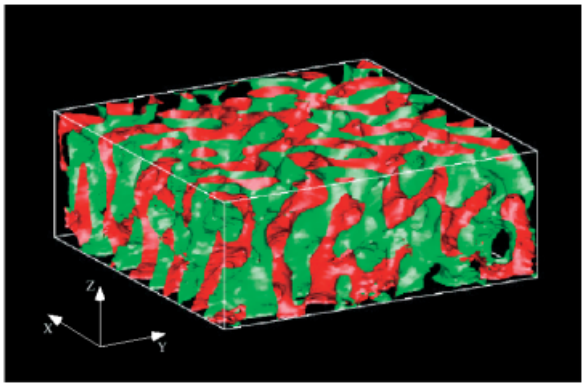

Fig. 4. 3D LSCM images of the interface shown over a larger scale than that in Fig. 3. The sample observed is the same as that in Fig. 3. The image has a volume of $80 \times 80 \times 30$ μm^3.

In order to confirm whether or not the 3D phase structure constructed with LSCM truly reflects a real structural entity, we calculated the scattering structure factor from the 3D digital image and compared it with the structure factor obtained from a TRLS experiment. For this purpose, we calculated scattering structure factor $S(q) \sim |\Psi(q)|^2$ where $\Psi(q)$ is the 3D Fourier transformation of the binarized 3D digital image where q is wavenumber. The results are shown in Fig. 5 where the scaled structure factor $S(q/q_m)$ obtained at various times at the late stage of SD of a 50/50 mixture of dPB (weight-average molecular weight M_w=1.43x10^5) and PB labelled with anthracene (PB-AN, M_w =9.5x10^5) by using fluorescent LSCM (black symbols) is compared with that obtained from TRLS (red symbols) (Ref. 14). Naturally, the structure factor obtained from TRLS is universal with time and, similarly, the structure factor obtained from LSCM is also universal with time. Moreover, it is quite impressive that two universal structure factors agree quite well over a large intensity scale, as large as five orders of magnitude, and a large spatial scale, as large as two orders of magnitude. Thus we conclude that the 3D LSCM image truly reflects the real structure entity. For the definition of the scaled structure factor, the reader is referred to Refs. 2-4, for example.

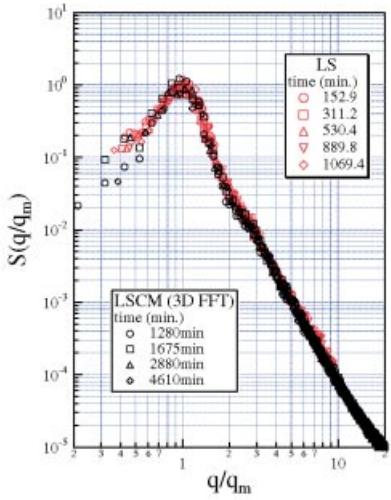

Fig. 5. Comparisons of scaled structure factors $S(q/q_m)$ obtained from the 3D LSCM image (black symbols, ○, □, △, ◇) and the TRLS experiments (red symbols, ○, □, △, ▽, ◇) for an isometric polymer mixture composed of dPB and PB-AN (PB labelled with anthracene). The variable q is the wavenumber of a Fourier mode of the structure or magnitude of scattering vector and q_m is q at which the structure factor $S(q)$ becomes maximum, i.e., the wave number for the dominant Fourier modes. ($q_m = 2\pi/\Lambda_m$, where Λ_m is average spacing or characteristic length of the structure.).

Figure 6 demonstrates time evolution of 3D structures observed for the 50/50 v/v mixture of dPB and PB-AN. It is shown that the sponge-like structure grows self-similarly: The scaled structure factors obtained from the 3D images constructed at different times at the late stage of SD are universal with time (see Fig. 5). Therefore, the shape of the sponge-like structure is universal with time but only the characteristic length scale $\Lambda_m = 2\pi/q_m$ increases with time according to the scaling law of $\Lambda_m \sim t$.

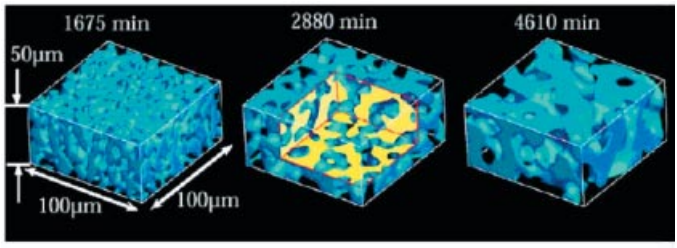

Fig. 6. Time evolution of sponge-like structure observed for dPB/PB labelled with anthracene (PB-AN): the 50/50 v/v mixture undergoing the late-stage spinodal decom-position. The PB-AN phase is blue, while the dPB phase is the empty space (by fluorescent laser scanning confocal microscopy).

What is the Physical Basis of Sponge-like Structure?

Having firmly established the 3D optical image of the sponge-like structure, we now address the question concerning the physical basis of the structure. For this purpose, we studied whether or not the structure can be predicted by a field theory called the time-dependent Ginzburg-Landau theory (TDGL) with hydrodynamic interactions (Ref. 7). The TDGL theory is based on a non-linear time evolution equation of the order of parameter field, i.e., spatial composition fluctuations of molecules A and B. Since the equation is non-linear and non-local, we cannot expect analytical solutions. Thus we solved the problem by 3D computer simulations. The detailed methodology and detailed comparison of the results obtained by simulations and scattering experiments were reported elsewhere (Refs. 7,15).

Figure 7 compares $S(q/q_m)$ obtained from the computer simulation (solid line) with that obtained from LSCM (shown by data points), showing again an excellent agreement with $S(q/q_m)$ obtained from the LSCM and TRLS experiments.

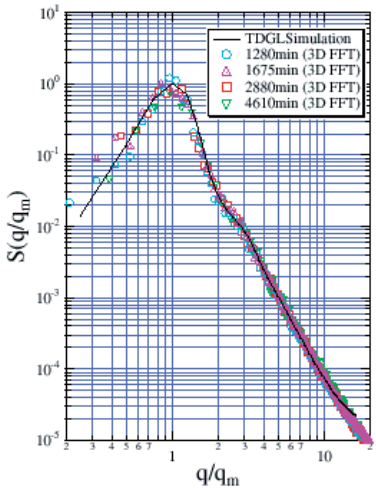

Fig. 7. Comparison of scaled structure factors $S(q/q_m)$ obtained from the 3D computer simulation with system size of 128^3 (solid line) with that obtained from the 3D LSCM image (data points ○, △, □, ▽).

The result thus demonstrates that the sponge-like structure is theoretically predictable: the sponge formation discussed here is driven by thermodynamic instability of the isometric systems. The simulated result was obtained for a reduced shear viscosity of $\dot{\eta}$ where $\dot{\eta}$ is the only relevant parameter in the TDGL model associated with hydrodynamic interactions and measures the inverse of the strength of the hydrodynamic interactions (Ref. 7). It was also elucidated that the shape of evolving structure, $S(q/q_m)$, is rather insensitive to the value of $\dot{\eta}$,

although the time evolution of the size of the structure $\Lambda_m(t) = 2\pi/q_m(t)$ is very sensitive to the value of $\dot{\eta}$ (Refs. 7,15). Molecular parameters and thermodynamic parameters such as temperature and pressure also affect the time evolution of the characteristic length Λ_m but the sponge structure scaled with Λ_m, i.e., the shape of the structure, is universal with these parameters. Thus we can conclude that the form of the evolving structures bears universality in the scaling regime.

Figure 8a shows a 3D image of the interface constructed by simulations for an isometric binary mixture at the late stage of SD, while Fig. 8b shows corresponding 2D sliced images demonstrating the time evolution of morphology. Note that features of the computer-simulated interface are quite similar to those constructed by LSCM, as is naturally expected from the identity in $S(q/q_m)$ shown in Fig. 7.

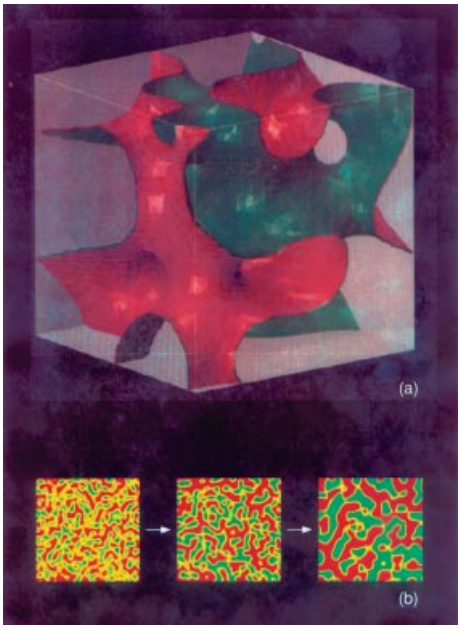

Fig. 8. 3D image of the interface constructed by computer simulations using (a) the TDGL model for an isometric binary mixture in the late-stage SD, and (b) 2D sliced images showing time evolution of the morphology (time elapsing from left to right). The edge length of the box in (a) corresponds to about 1.5 Λ_m.

The TDGL model is quite general, applicable to all mixtures of small molecules as well as polymer molecules. When the model is applied to polymer mixtures, the two polymers are assumed to have equal static and dynamic properties, i.e., polymer pairs being "symmetric", having nearly equal molecular weights and viscosities. The real polymer mixtures used in

this study are also symmetric in this sense. The scaled structure factors obtained for such symmetric polymer mixtures were shown to be essentially identical to those obtained for simple liquid mixtures (Refs. 4,16) and metalic alloys (Ref. 2). Thus the sponge-like structure shown in Figs. 3, 4 and 6 is universal for any phase-separating isometric mixtures via the SD process. Thus we succeeded for the first time in visualizing the real-space images of spinodally decomposed bicontinuous two-phase structures for simple liquid mixtures, metalic alloys and inorganic glasses, etc. by using polymer mixtures as model systems.

How Can the Sponge-like Structures Be Characterized and Analyzed Mathematically?

Now that we have determined the 3D structure, which accurately reflects real structures from the global to local scale, and that we have obtained a sound physical basis for this structure, we proceed to analyze the structure in terms of interface curvatures, based on differential geometry. We first used the "parallel surface method" to determine the area-averaged mean curvature $\langle H \rangle$ and Gaussian curvature $\langle K \rangle$,

$$A(d) = A_0 (1 + 2 \langle H \rangle d + \langle K \rangle d^2) \qquad (1)$$

where A_0 is interface area, and $A(d)$ is the area of the surface which is parallel to and located at a distance d from the interface. H and K are local mean curvature and Gaussian curvature defined earlier in the caption to Fig. 1.

We used the "marching-cube algorithm" (Ref. 17) to construct the 3D interface structure in that the interface is composed of triangles, as schematically shown in Fig. 9a. To construct the parallel surface at a displacement vector $\boldsymbol{d}$ ($|\boldsymbol{d}| = d$) from the interface, we first calculate normal vectors $\boldsymbol{n}$ ($|\boldsymbol{n}| = 1$) at the vertices of the triangles (red arrows), as will be detailed elsewhere (Refs. 18,19). Then $\boldsymbol{d}$ is given by $\boldsymbol{d} = d\boldsymbol{n}$, and the parallel surface, composed of yellow triangles as shown in Fig.9b, is constructed by connecting the ends of the displacement vectors. $A(d)$ is then calculated by summing the areas of the triangles.

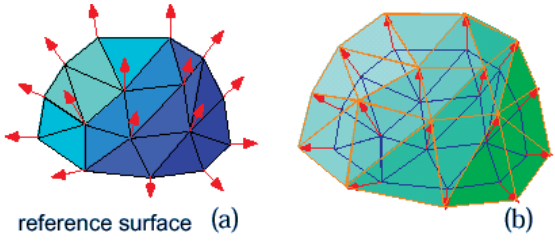

Fig. 9. Schematic representation of (a) the interface (blue reference surface) composed of triangles and normal vectors (red arrows) at their vertices and (b) the parallel surface constructed by connecting the normal vectors.

The best fit of the results of $A(d)$ obtained from the 3D images shown in Figs. 3 and 4 with Eq. 1 yielded (Ref. 19)

$$A_0/V = 2.2 \times 10^{-1}\ \mu m^{-1},$$

$$\langle H \rangle = 7.0 \times 10^{-3}\ \mu m^{-1},$$

$$\langle K \rangle = -6.2 \times 10^{-2}\ \mu m^{-2}\ (\text{or } [-\langle K \rangle]^{1/2} = 2.5 \times 10^{-1}\ \mu m^{-1}),$$

where A_0/V is the interface area per unit volume. These parameters depend on time, and the absolute values definitely decrease with time (Ref. 19). We can also conclude that the sponge-like structure has a hyperbolic interface having a negative area-averaged Gaussian curvature $\langle K \rangle$ and almost zero area-averaged mean curvature $\langle H \rangle$, i.e., $r \equiv \langle H \rangle / [-\langle K \rangle]^{1/2} \cong 0$. The small positive value of r (ca. 0.03) may reflect portions of bicontinuous domains having cylinder-like structures which tend to burst during the domain growth.

The time evolution of these characteristic parameters has been analyzed as well (Ref. 19). It is intriguing to note that $r \cong 0$, irrespective of time during the self-organization process. This may be the most rational path taken by the evolving structures in the isometric systems. The fact that $\langle H \rangle$ is close to zero does not necessarily mean that the interface of the evolving non-equilibrium domains is close to minimal surface. To understand this point, one must determine distribution functions of the local curvatures H and K. We have attempted to determine the distributions both from the 3D optical images (Ref. 20), also based on a principle of differential geometry, and from the 3D computer simulations (Ref. 21). The results revealed that the distribution of H for our interface is broader than that for the periodic minimal surface of gyroid, for example, implying distortions of our interface from the ideal mathematical minimal surface.

The area-averaged curvatures $\langle H \rangle$ and $\langle K \rangle$ and the distributions of the curvatures from the mean values determined from the 3D optical images are found to be consistent with the so-called "scattering-mean-curvature" obtained from scattering experiments (Refs. 13,22), based on the Kirste-Porod-Tomita theory (Refs. 23,24). This evidence further reinforced the merit of our approach presented here in two senses: (i) it supports the scattering theory and proves that the scattering method provides a particular moment of the curvature distributions which we designate "scattering-mean-curvature" $\langle K_S^2 \rangle \equiv (3 \langle H^2 \rangle - \langle K \rangle) / 2$; (ii) it further supports the accuracy of our methods and analyses because the scattering method is essentially independent of the present method in terms of the curvature determination.

How Universal Could The Sponge-like Structures Be?

We have already noted that the sponge-like structure found for the spinodally decomposed symmetric polymer mixtures is universally applied to bicontinuous structures developed for critical mixtures of small molecules or atoms via the SD processes. In order to further address this question, we compare the bicontinuous structures in microemulsion systems, e.g., a ternary mixture of heavy water (D_2O), *n*-octane, and tetraethylene glycol monodecyl ether (C_{10}-E_4, a non-ionic surfactant) at the hydrophile-lipophile balance (HLB) temperature, with those in our simple molecular mixtures composed of hydrocarbon polymers. The microemulsion system also forms structures similar to those in the polymer mixtures, i.e.,

isometric bicontinuous domains of water and oil with most of the surfactant molecules at the interface, despite the fact that intermolecular interactions in the system are more complex than those in polymer mixtures. It should be noted here that the bicontinuous structures in the microemulsion systems are equilibrium structures, while those formed via the SD processes are nonequilibrium ones.

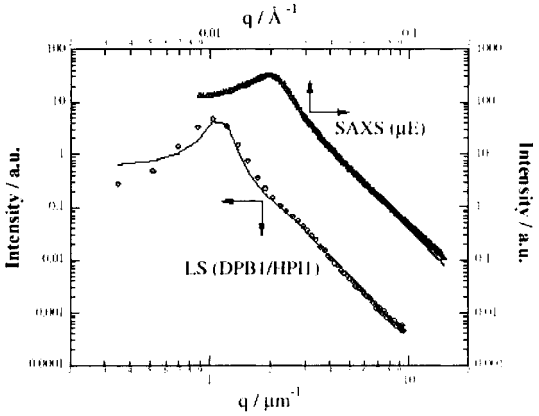

Fig. 10. Comparison of the SAXS function from the equilibrium isometric microemulsion system at the HLB point (μE) with the TRLS function from the isometric polymer mixture at a particular time in the late-stage SD (both shown by data points (Ref. 25)). The solid lines are the best fit with the RGW theory.

Figure 10 shows a small-angle X-ray scattering (SAXS) function from the microemulsion system (triangles) together with TRLS functions (circles) from the isometric polymer mixture at the late stage of SD (Ref. 25). The solid lines show the best fits of the random Gaussian wave (RGW) theory (Refs. 26,27) for the experimental scattering functions. The theory assumes a suitable form of the spectral function $f(k)$ which is an inverse sixth-order polynomial in wavenumber k and which is an extension of the well-known structure factor proposed by Teubner and Strey (Ref. 28). The scattering function as well as the real-space structure can be calculated from $f(k)$.

We choose the following approach in order to extract useful information about the structures occurring in the systems in the context of the RGW theory. The best fit of the calculated scattering function for the experimental scattering function determines $f(k)$, and the $f(k)$ in turn determines important physical parameters such as an average spacing of the structure, Λ_m, the coherence length of the local order, ξ (Ref. 29), and $\langle K \rangle$ (Ref. 25) as well as the real-space structures. The real-space structures thus determined are shown in Fig. 11.

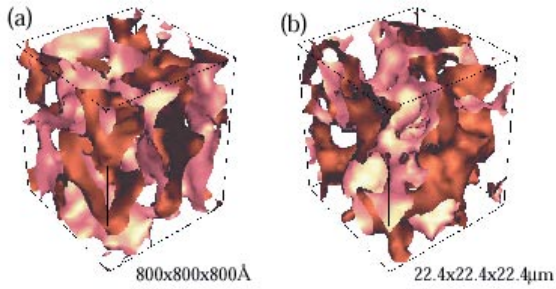

Fig. 11. 3D image of the interfaces constructed on the basis of Gaussian random wave theory: (a) for an isometric microemulsion system at the HLB point and (b) for an isometric mixture at the late stage of SD (Ref. 25).

At first glance, the two profiles shown in Fig. 11 are very similar, except for the absolute length scales (about 10 nm vs. 1 μm). Similarly, the two real-space structures constructed on the basis of the RGW theory show a striking resemblance, having sponge-like characteristics (see Fig. 11). The real-space structures constructed using the RGW theory are expected to reflect real structural entities because of good agreement with the theoretical and experimental scattering functions.

Quantitative comparisons of the two systems are summarized in Table 1. Note the similarity of the two sponge-like structures in the reduced Gaussian curvature $[-\langle K\rangle]^{1/2}/q_m$ on a quantitative basis as well. Again, we should note that the values of $\langle K\rangle$ thus estimated are negative for the two structures. An important difference in the two structures is discernible in the reduced coherence length, ξ/Λ_m. The polymer system has a larger coherence length (a higher degree of the long-range order) than the microemulsion system. This aspect is manifested by the fact that the low-q part of $I(q)$ in the polymer system cannot be fitted well by the theoretical scattering function as shown in Fig. 10. This point raises an important question in theoretical physics of the RGW theory when it is applied to polymer systems with a seemingly smaller random thermal noise effect compared with the low-molecular-weight microemulsion system. In this regard, the TDGL theory gives a better prediction than the RGW theory.

Table 1. Comparison of sponge-like structures in the microemulsion system and the polymer mixture (polymer).

Physical quantity	Polymer	Microemulsion	Polymer/ microemulsion[a]
q_m[b]	1 μm^{-1}	2×10^{-2} $Å^{-1}$	5×10^{-3}
Λ_m[b]	6.28 μm	3.14×10^2 Å	2×10^2
$[-<K>]^{1/2}$	1.44 μm^{-1}	1.07×10^{-2} $Å^{-1}$	4×10^{-3}
$[-<K>]^{1/2}/q_m$	0.44 (0.48[c])	0.54	0.8 (0.9[c])
ξ/Λ_m[d]	1	0.6	1.7

[a] The ratio of a physical quantity for polymer and that for microemulsion; [b] $q_m = 2\pi/\Lambda_m$ where q_m and Λ_m are the characteristic wavenumber and length, respectively; [c] the value for the polymer mixture as determined by direct real-space analysis; [d] reduced coherence length.

Concluding Remarks

We have constructed three-dimensional (3D) real-space images of bicontinuous domain structures in phase-separating polymer mixtures via spinodal decomposition (SD). The 3D images exhibit "sponge-like" structures. They were found to provide a visualized model for the universal scaled structure factors established for critical mixtures of symmetric polymer molecules, small molecules or atoms undergoing the late-stage process of SD. The sponge-like structures well predictable by the nonlinear time-evolution equation based on the TDGL theory are universal for systems with thermodynamic instability which phase-separate into bicontinuous domains with well-defined interface. They compose of saddle-shape interfaces with negative area-averaged Gaussian curvature $<K>$ and almost zero area-averaged mean curvature $<H>$.

Acknowledgements

The authors thank Dr. S-H. Chen and Dr. S.T. Hyde for their collaborations and enlightening comments.

References

1. J.W. Cahn, *J. Chem. Phys.* **1965**, 42, 93.
2. See, e.g., J.D. Gunton, M. San Miguel, and P.S. Sahni, in *Phase Transitions and Critical Phenomena*, (C. Domb and J.L. Lebowitz, Eds.), Academic Press, New York, **1983**, pp. 269-482; K. Binder, in *Materials Science and Technology*, (R.W. Cahn, P. Haasen, and E.J. Kramer, Eds.), Vol. 5 *Phase Transformations in Materials*, VCH, Weinheim, **1991**, pp. 143-212; S. Komura and H. Furukawa, *Dynamics of Ordering Processes in Condensed Matter*, Plenum, New York, **1988**.
3. T. Hashimoto, in *Materials Science and Technology*, (R.W. Cahn, P. Haasen, and E.J. Kramer, Eds.), Vol. 12, *Structure and Properties of Polymers*, VCH, Weinheim, **1993**, pp.251-300.
4. T. Hashimoto, *Phase Transitions* **1988**, 12, 47.
5. See, e.g., H. Furukawa, *J. Phys. Soc. Jpn.* **1989**, 58, 216.
6. A. Shinozaki and Y. Oono, *Phys. Rev. E* **1993**, 48, 2622.
7. T. Koga and K. Kawasaki, *Physica A* **1993**, 196, 389.

8. T. Hashimoto, H. Jinnai, H. Hasegawa, and C.C. Han, *Physica A* **1994**, 204, 261.
9. K. Binder and D. Stauffer, *Phys. Rev. Lett.* **1974**, 33, 1006.
10. See, e.g., T. Wilson, *Confocal Microscopy*, Academic Press, London, **1990**, pp. 1- 64.
11. A. Ribbe and T. Hashimoto, *Macromolecules* **1997**, 30, 3999.
12. S. Hyde, S. Anderson, K. Larsson, Z. Blum, T. Landh, S. Lidin, and B.W. Ninham, *The Language of Shape*, Elsevier, Amsterdam, **1997**.
13. T. Hashimoto, H. Jinnai, Y. Nishikawa, T. Koga, and M. Takenaka, *Prog. Colloid Polym. Sci.***1997**, 106, 118.
14. T. Hashimoto, T. Koga, H. Jinnai, and Y. Nishikawa, *Nuovo Cimento Soc. Ital. Fis., D* **1998**, 20, 1947.
15. T. Koga, K. Kawasaki, M. Takenaka, and T. Hashimoto, *Physica A* **1993**, 198, 473.
16. M. Takenaka and T. Hashimoto, *J. Chem. Phys.* **1992**, 96, 6177.
17. W. E. Lorensen and H. E. Cline, *Computer Graphics SIGGRAPH'87* **1987**, 21, 163.
18. Y. Nishikawa, H. Jinnai, T. Koga, T. Hashimoto, and S.T. Hyde, *Langmuir* **1998**, 14, 1242.
19. H. Jinnai, Y. Nishikawa, T. Koga, T. Hashimoto, and S.T. Hyde, *Phys. Rev. Lett.* **1997**, 78, 2248.
20. Y. Nishikawa, T. Koga, T. Hashimoto, and H. Jinnai, *Langmuir* **2001**, 17, 3254.
21. T. Koga, H. Jinnai, and T. Hashimoto, *Physica A* **1999**, 263, 369.
22. M. Takenaka and T. Hashimoto, *Physica A*, **2000**, 276, 22.
23. B. Kirste and G. Porod, *Kolloid-Z. Z. Polym.* **1962**, 184, 1.
24. H. Tomita, *Prog. Theor. Phys.* **1984**, 72, 656.
25. H. Jinnai, T. Hashimoto, D.D. Lee, and S.H. Chen, *Macromolecules* **1997**, 30, 130.
26. N.F. Berk, *Phys. Rev. Lett.* **1987**, 58, 2718.
27. S.H. Chen, D.D. Lee, and S.L.Chang, *J. Mol. Struct.* **1993**, 296, 259.
28. M. Teubner and R. Strey, *J. Chem. Phys.* **1987**, 87, 3195.
29. S.H. Chen, S.L. Chang, and R. Strey, *J. Appl. Crystallogr.* **1991**, 24, 721.